UCLA
UCLA Previously Published Works

Title
Ru-Catalyzed Hydrogenolysis of Methanol: A Computational and Kinetics Study

Permalink
https://escholarship.org/uc/item/8163g0z5

Journal
ChemCatChem, 15(9)

ISSN
1867-3880

Authors
Sackers, Nina M
Nikodemus, Julia
Palkovits, Regina
et al.

Publication Date
2023-05-05

DOI
10.1002/cctc.202201530

Copyright Information
This work is made available under the terms of a Creative Commons Attribution-NonCommercial-NoDerivatives License, availalbe at https://creativecommons.org/licenses/by-nc-nd/4.0/

Peer reviewed

eScholarship.org Powered by the California Digital Library
University of California

RESEARCH ARTICLE

Ru-Catalyzed Hydrogenolysis of Methanol: A Computational and Kinetics Study

Nina M. Sackers,[a] Julia Nikodemus,[a] Regina Palkovits,[a] Philippe Sautet,[b, c] and Peter J. C. Hausoul*[a]

[a] Nina M. Sackers, Julia Nikodemus, Prof. Dr. Regina Palkovits, Dr. Peter J. C. Hausoul
Chair of Heterogeneous Catalysis and Technical Chemistry
RWTH Aachen University
Worringerweg 2, 52074 Aachen, Germany
E-mail: Hausoul@itmc.rwth-aachen.de
[b] Prof. Philippe Sautet
Department of Chemical and Biomolecular Engineering
University of California, Los Angeles
Los Angeles, California 90095, United States
[c] Prof. Philippe Sautet
Department of Chemistry and Biochemistry
University of California, Los Angeles
Los Angeles, California 90095, United States

Supporting information for this article is given via a link at the end of the document.

Abstract: In spite of numerous kinetic studies, the mechanism of the polyol hydrogenolysis on a Ru catalyst surface is still not fully understood. Here, the decomposition of the C_1 alcohol methanol can serve as an entry to the clarification of the mechanism. Therefore, kinetic experiments using a Ru/C catalyst and periodic DFT calculations on a Ru(0001) model surface were performed. A modeling of the Ru surface revealed that the surface is most likely covered with hydrogen adsorbates under experimental conditions. On a clean Ru model surface, the overall activation barrier is lower if less dehydrogenation steps occur on the substrate methanol before the C-O bond cleavage. Transferring the results from the clean to the hydrogen-saturated Ru surface, the pathway via CH_2O O-H formation and subsequent C-O cleavage is found to be the most favorable. This study shows that the surface coverage has a significant influence on the activation barrier.

Introduction

The depletion of fossil carbon feedstocks as well as concerns about their environmental impact demand the employment of alternative resources. Biomass is one promising and abundant carbon source that can be utilized for the CO_2-neutral production of chemicals and fuels.[1] Lignocellulosic biomass in particular holds the advantage of low cost and noncompetitiveness with food plants. The cellulosic and hemicellulosic fractions of biomass can efficiently be converted to C_6 and C_5 polyalcohols, respectively, by combining acid-catalyzed hydrogenolysis with metal-catalyzed hydrogenation. Further hydrogenation performed at elevated temperatures in the presence of metal catalysts leads to short-chained polyols by hydrogenolytic C-C and C-O bond scission (Scheme 1).[2] These polyalcohols find wide applications as building blocks in polymer synthesis, in pharmaceutical industry and as additives in food industry.[2a] Even though in heterogeneous catalysis various and extensive experimental studies on the hydrogenolysis of polyols were carried out, the molecular reaction on the catalyst surface is yet not fully understood. Computational chemistry can be a helpful tool to gain mechanistic insights on the polyol reactivity on catalytically active metal surfaces.[3]

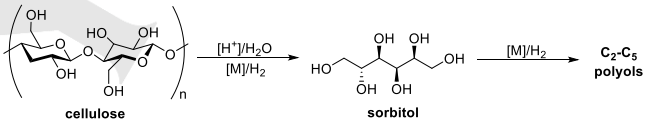

Scheme 1. Formation of C_2-C_5 polyols from cellulose.

The mechanism of the hydrogenolysis of polyols has been investigated extensively.[4] In particular, two publications by our group elucidate the polyol decomposition performed on a Ru catalyst under neutral reaction conditions.[5] Here, sorbitol, xylitol and erythritol were converted in the presence of Ru/C and molecular hydrogen towards various polyols comprising hexitols, pentitols, tetritols, triols and diols. Based on the experimental results, stereoisomerization, decarbonylation and deoxygenation were proposed as the three main decomposition pathways (Scheme 2). These reactions take place simultaneously on the substrate and all of the subsequent products. Within the stereoisomerization (Scheme 2, a), it is generally accepted that one of the hydroxy groups connected to a stereocenter changes its configuration by reversible (de)hydrogenation via successive O-H and C-H cleavage reactions to a carbonyl species.[6] The C-C bond scission between a terminal and an adjacent carbon atom is referred to as decarbonylation and results in a polyol that is shortened by one carbon atom (Scheme 2, b). It is probably initiated by dehydrogenation of the polyol towards an aldehyde.[4f] A polyol exhibiting one hydroxy group less at a terminal position can be obtained by C-O bond cleavage in a deoxygenation step (Scheme 2, c). The experimental evidence on the deoxygenation reaction revealed the racemization of one stereocenter, therefore it was proposed that this reaction could occur via the formation of an enol and a ketone, subsequently. In general, a fourth

decomposition pathway leading to C-C bond scission at any position in the carbon chain is described by several authors and denoted as a retro-aldol mechanism.[4a, 4e] However, the applied Ru/C catalyst cannot catalyze this reaction under the given neutral conditions and therefore, this mechanism was not observed in the studies.[5]

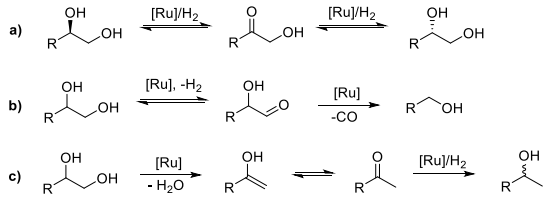

Scheme 2. Proposed schematic Ru/C-catalyzed polyol decomposition pathways. a) Stereoisomerization, b) decarbonylation, c) deoxygenation.[5a]

Based on the C_1 alcohol methanol, we herein report a model study on the decomposition mechanism using computational chemistry. As methanol contains a hydroxy group, which is one of the main characteristics of polyols, we elucidate the reaction mechanism under realistic reaction conditions including solvation effects and the coverage of the catalyst surface and compare computational results to our experimental findings. In contrast to current publications, we investigate the methanol decomposition towards methane, which is in line with our experimental results.

To date, computational studies regarding the hydrogenolysis of polyols and also the Ru-catalyzed decomposition of poly- and monoalcohols in particular are scarce. On Ru surfaces, only publications dealing with the methanol decomposition exist. The works by García-Muelas et al.[7] and Moura et al.[8] describe the formation of CO from methanol on a clean Ru(0001) surface. Both studies report quite similar results. The alcohol H activation towards methoxy was identified as the first reaction step, even though García-Muelas et al. found a lower activation barrier for the methanol C-H cleavage. Since the alkoxide species has a significantly higher thermodynamic stability and only methoxy is observed experimentally[9], they state the decomposition pathway via methoxy as predominant. Subsequent C-H scissions yield CO and molecular hydrogen as the final products. In the work of García-Muelas et al.[7] CO is formed via successive C-H cleavage reactions from H_2CO, whereas according to Moura et al.[8] the same reaction occurs in one step. In both publications, the methoxy C-H cleavage demands the highest activation barrier between 61 and 87 kJ mol^{-1}. On the contrary, the steps regarding the formation of CO from formaldehyde require only minimal activation energy (0 – 6 kJ mol^{-1}). Further publications partly deal with the aforementioned steps of the methanol decomposition.[10] These studies confirm the low activation barriers found for the formaldehyde and formyl C-H cleavages. However, in all these publications the reaction was investigated on a clean Ru surface in vacuum conditions. Based on the work of García-Muelas et al.[7], the same group analyzed the effects of solvation in water on the reaction by applying an implicit solvation model combined with two explicit solvent molecules.[11] Due to proton transfer to the water adsorbate, the methoxy formation requires no activation energy and the activation barrier of the methoxy C-H bond cleavage is lowered by 16 kJ mol^{-1}. Regarding the methanol decomposition, no studies consider interactions with other adsorbates except water.

Several publications study the effect of solvation and surface coverage on the reactivity of polyols. When water is used as a solvent, the metal catalyst exhibits a wetting layer caused by adsorption of water molecules.[12] Therefore, wet surfaces cannot be modeled by a vacuum/metal interface. Michel et al. found that in the presence of another water or alcoholic substrate molecule the formation of a hydrogen-bonded dimer is usually more favorable than generating an additional metal-O bond.[13] This facilitates the O-H bond scission for the weakly adsorbed hydrogen bond acceptor due to preorganization of the transition state (TS). On the contrary, the C-H bond cleavage is slightly inhibited by this effect. Furthermore, Sinha et al.[10c] stated that higher surface coverages of the substrate and hydrogen would result in lateral repulsive interactions and consequently, decrease the activation barriers for hydrogenation.

In the following we present a kinetic analysis of the hydrogenolysis of methanol over Ru/C at different temperatures and the obtained apparent activation energies. Subsequently the reaction pathways are studied comprehensively using periodic DFT on a Ru(001) surface with implicit solvation on a clean and hydrogen covered surface, to obtain reaction pathways with the lowest energetic spans. Finally the experimental and theoretical results are compared.

Results and Discussion

Kinetics of the Ru/C-Catalyzed Hydrogenolysis of Methanol

Hydrogenolysis experiments of methanol were performed in an aqueous solution using a Ru/C catalyst in the presence of high pressures of molecular hydrogen. Prior to the kinetic measurements, blank experiments without catalyst were performed and proved the necessity of the catalyst for the hydrogenolysis reaction. The experimental hydrogenolysis of methanol led to methane as the only decomposition product (Figure S1). Consequently, other possible products or intermediates such as CO and CO_2 were not generated or completely hydrogenated on the Ru catalyst. The kinetics of the methanol decomposition to methane was studied by determining the pseudo-first order rate constant k_{mm} from the methanol concentrations at different reaction temperatures (Figure 1, left). The second order rate constant k was obtained by taking into account the experimentally measured Ru dispersion of 0.175 of the Ru/C catalyst in the catalyst concentration. Thereof, the apparent activation enthalpy $\Delta H^{\ddagger}_{app}$, the entropy of activation $\Delta S^{\ddagger}_{app}$ and the Gibbs energy of activation $\Delta G^{\ddagger}_{app}$ were calculated using the Eyring method (Figure 1, right).[14]

The methanol hydrogenolysis to methane on Ru/C has a $\Delta H^{\ddagger}_{app}$ of about 110 kJ mol^{-1} (Table 1). This value is in the same order of magnitude as other apparent activation enthalpies for the decarbonylation and deoxygenation on the same catalytic system. Our group found a $\Delta H^{\ddagger}_{app}$ of 118 kJ mol^{-1} and 122 kJ mol^{-1} for the first decarbonylation of xylitol and sorbitol, respectively. Furthermore, the deoxygenation of xylitol has a $\Delta H^{\ddagger}_{app}$ of 83 kJ mol^{-1}.[5b] However, these results are hardly comparable since the C_5 and C_6 polyols have far more possibilities for interactions with the catalyst surface due to their several hydroxy groups.

The experimental $\Delta G^{\ddagger}_{app}$ of 115 kJ mol^{-1} is very similar to $\Delta H^{\ddagger}_{app}$ since the value of $\Delta S^{\ddagger}_{app}$ is quite low (Table 1). This

experimentally determined Gibbs energy of activation serves as a reference for the computational results.

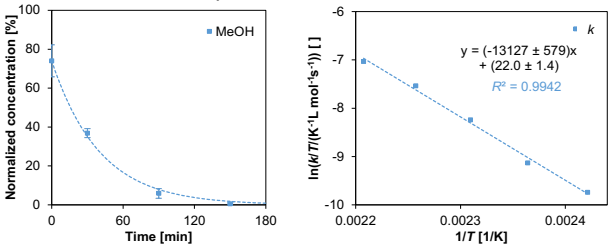

Figure 1. Ru-catalyzed decomposition of methanol (conditions: 0.525 g MeOH, 0.400 g Ru/C (5 *wt.*%), 20 mL H_2O, 170 °C, 80 bar H_2) (left) and Eyring regression of the decomposition (right).

Table 1. Summary of the Eyring regression and thermodynamic quantities of the methanol hydrogenolysis.

Quantity	Value
Slope	-13127 ± 579
Intercept	22.0 ± 1.4
$\Delta H^{\ddagger}_{app}$ [kJ mol^{-1}]	109 ± 5
$\Delta S^{\ddagger}_{app}$ [J mol^{-1} K^{-1}]	-14.5 ± 11.2
$\Delta G^{\ddagger}_{app}$ [kJ mol^{-1}]	115 ± 10

Modeling of the Most Stable Ru Surface

Since under experimental conditions the Ru catalyst surface is not clean but covered with adsorbates like the substrates methanol and hydrogen as well as the solvent water, the most stable and thus, the most probable surface has to be identified. Methanol is preferably adsorbed by dissociation of the O-H bond to methoxy and hydrogen (Figure 2, a). This corresponds to a coverage of 2/9 monolayer (ML), as two adsorption sites are occupied in a cell with 9 Ru surface atoms. As a cell with 9 Ru surface atoms has 9 fcc threefold hollow sites, which are preferred for the investigated substrates, 9 sites are used as a reference for adsorption sites. At a coverage of 2/9 ML, a stabilization by G_{ads} = 83 kJ mol^{-1} is reached under the given reaction conditions (Table 2, a). A higher coverage, however, destabilizes the adsorption probably due to steric repulsion between the methyl groups (Figure S3, a). A lower stabilization of 37 kJ mol^{-1} is obtained when three intact methanol molecules are adsorbed on a 3x3 Ru cell (1/3 ML) (Figure S3, b).

Due to lower steric demands, water can be bound with a significantly higher coverage of 6 water molecules per 9 Ru atoms (2/3 ML), which is denoted as a bilayer.[12] The most stable arrangement of water on a 3x3 Ru slab is a partially dissociated bilayer (Figure 2, b), which reaches a stabilization of 110 kJ mol^{-1} (Table 2, b). This finding is in line with computational and experimental findings.[12, 15]

Molecular hydrogen adsorbs preferably dissociatively on fcc threefold hollow sites with a maximum coverage of 1 ML of H,[16] which can be confirmed by our results showing an energy stabilization of 398 kJ mol^{-1} (Table 2, c). However, the adsorption energies for the fcc and hcp threefold hollow sites deviate only slightly and consequently, both adsorption modes are feasible.

Probing surfaces mixed with different adsorbates revealed that a (3x3) slab composed of one water molecule and seven hydrogen adsorbates has the highest stability (Table 2, d), though it is less favored than the hydrogen-saturated surface. Accordingly, the ruthenium slab has an energy minimum, if all fcc threefold hollow sites are occupied with hydrogen atoms.[17] Therefore, this structure will be regarded as the starting point of the reactions.

Table 2. Adsorption Gibbs free energies of methanol, water, hydrogen and mixed water and hydrogen saturated on a (3x3) Ru slab. Adsorbed atoms are indicated by an asterisk.

Reaction	ΔG_{ads} [kJ mol^{-1}]
a) $H_3C{-}OH_{(aq)} + Ru_{(3x3)} \rightarrow H_3CO^* + H^*$	-83
b) $6\ H_2O_{(aq)} + Ru_{(3x3)} \rightarrow 3\ H_2O^* + 3\ ^*OH + 3\ H^*$	-110
c) $4.5\ H_{2\,(g)} + Ru_{(3x3)} \rightarrow 9\ H^*$	-398
d) $3.5\ H_{2\,(g)} + H_2O_{(aq)} + Ru_{(3x3)} \rightarrow 7\ H^* + H_2O^*$	-325

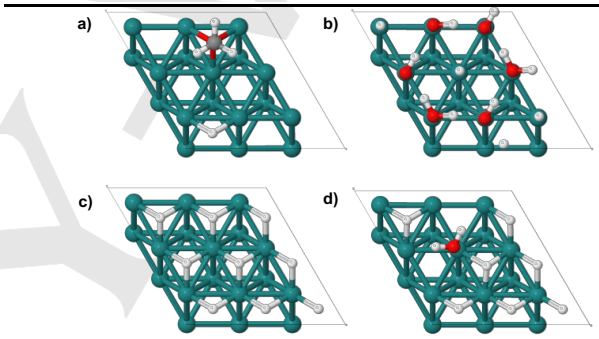

Figure 2. Front view of the most stable adsorption geometries of a) methanol, b) water, c) hydrogen and d) mixed water and hydrogen saturated on a (3x3) Ru slab. Color code: Ru = teal, O = red, C = gray, H = white.

In analogy with Pd-H hydrides[18], the incorporation of hydrogen atoms in the Ru lattice could be possible, but to our knowledge no publications regarding Ru-H hydrides are present. This is supported by calculations showing that the incorporation of H in the Ru(0001) slab is unfavorable (Table S2).

Mobility of Adsorbates on the Ru Catalyst Surface

Even though the Ru catalyst surface fully covered with H adsorbates is the thermodynamic energetic minimum, metastable energetic states with vacant adsorption sites will be present under the given reaction conditions (ϑ > 150 °C, ϑ: temperature). However, an identification of the actual coverage of hydrogen on the surface would require kinetic modelling using Kinetic Monte Carlo simulations. Nevertheless, in order to ensure the most favorable coverage of H atoms on the investigated slab, the mobility of adsorbed H atoms on the Ru catalyst surface was investigated. By this means, hydrogen atoms could migrate into the slab to fill vacant sites after consumption of hydrogen atoms in hydrogenation steps or they could migrate into a neighboring slab, if an additional vacancy is required for a bond cleavage. The migration of hydrogen from one fcc threefold hollow site to another takes place via a local minimum on a hcp threefold hollow site. The transition states connecting these minima are located on the

bridge sites between those hollow sites (Figure S5). The barrier for migration ($\Delta E_{mig}^{\ddagger}$) of H atoms on a clean Ru(0001) surface amounts to only 14 kJ mol^{-1} (Table 3). In addition, the barrier for migration of vacant sites on an almost fully H-covered surface is very similar (21 kJ mol^{-1}), since lateral interactions are small (Figures S6-7).

Furthermore, the mobility of the oxygen containing products of the hydrogenolysis was tested. If O and OH adsorbates have low migration barriers on the Ru surface, the hydrogenation of the C and O fragments can be treated separately, since migration between neighboring surface unit cells is possible. While the migration of OH requires a similarly low activation energy as the H atom, the barrier for migration of O is significantly higher and migration between different threefold hollow sites would be slow (Table 3). Consequently, we can assume that the oxygen atom remains on its adsorption site until being hydrogenated. However, O atoms adsorbed in proximity to a carbonaceous fragment have only a minor influence on the activation barrier of the C-H bond formation (cf. Table S3).

Table 3. Barrier for migration ($\Delta E_{mig}^{\ddagger}$) of H, O and OH on a clean and for vacancy migration on an almost fully H-covered Ru(0001) surface.

Adsorbate	$\Delta E_{mig}^{\ddagger}$ [a] [kJ mol^{-1}]
H	14
O	64
OH	20
vacancy	21

[a] Difference in electronic energy only and without dispersion corrections.

Methanol Decomposition Mechanisms on a Clean and a Hydrogen-Saturated Ru(0001) Surface

The mechanism of the methanol hydrogenolysis is investigated on both a clean and a hydrogen-saturated Ru(0001) model surface since the calculations are significantly simplified on the clean surface. Theoretically possible products of the decomposition reaction of methanol are either carbon monoxide, carbon dioxide or methane (Scheme 3). However, in our hydrogenolysis experiments of methanol on Ru/C methane was the only decomposition product (see Figure S1). Besides, the formation of methane is the only reaction that shows a negative Gibbs free energy (Scheme 3). Therefore, we focus on reaction pathways leading to methane in this study, which is in contrast to previous works on the methanol decomposition.[7-8] The most stable adsorption sites and geometries of all reactants, reaction intermediates and products were identified (Table S1) and this knowledge was considered in the computation of the catalytic cycles.

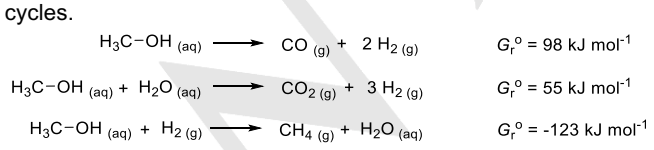

Scheme 3. Possible reactions for methanol decomposition. Gibbs free reaction energies were calculated at 150 °C and 80 bar.

A combination of dehydrogenation and hydrogenation reactions at the carbon and oxygen atom as well as the cleavage of the C-O bond are necessary to convert methanol into methane (Scheme 4). Since experiments revealed that methoxy is the predominantly adsorbed species on the Ru catalyst surface, it is very likely that the reaction sequence of the methanol decomposition starts with an O-H bond cleavage to methoxy.[9, 19] Therefore, reaction pathways via methanol C-O and C-H bond cleavages are not considered. In general, the C-O bond scission can take place at any dehydrogenation stage of methanol. The direct C-O cleavage of these intermediates as well as the C-O cleavage after an O-H formation can be distinguished (Scheme 4). After cleavage of the C-O bond, the obtained fragments are stepwise hydrogenated to methane and water. As C-H bond formations were found to have lower activation barriers than O-H bond formations (Table S3), the hydrogenation of carbonaceous fragments is considered before the formation of water. All reaction pathways (note: all pathways start at I and end at VI) presented in Scheme 4 were calculated on a clean Ru(0001) surface. As these are preliminary studies for the mechanism on a hydrogen-saturated Ru surface, dispersion interactions were neglected. The respective energy profiles and images of the stationary points can be found in the Supporting information (Figures S8-18). The mechanism of the complete dehydrogenation of methanol to CO coincides with the pathways discussed in the literature (Figure S16).[7-8] Comparably high activation barriers for the methanol O-H and the methoxy C-H cleavage were found, while the C-H bond scissions of formaldehyde and formyl have likewise minor activation barriers (cf. Table S3).

The barrier of the C-O bond scission in the different reaction pathways depends on the weakening of the C-O bond. It is significantly decreased, if the C-O cleavage takes place after formation of an O-H bond (Table S3). Moreover, C-O bond cleavages at earlier dehydrogenation stages feature lower activation barriers as the C-O bond is also weakened compared to CO. This weakening of the C-O bond can be confirmed by the increased C-O bond distances at earlier dehydrogenation stages in Figure 3 a) to d) and by longer C-O bonds after O-H bond formation of the respective intermediates (Figure 3 e) to g). The CH_3O C-O cleavage (II-III) however is less favorable, which is probably due to the steric hindrance of the methyl group (Figure S9).

In all considered pathways, the formation of O-H bonds needs considerably high activation energies between 100 kJ mol^{-1} and 166 kJ mol^{-1}, while C-H bond formations have lower activation barriers between 46 kJ mol^{-1} and 79 kJ mol^{-1} (Table S3). The reason for these relatively high barriers could be that the formation of O-H and C-H bonds requires the detachment of Ru-H bonds, similar to the formation of H_2, which already requires 38 kJ mol^{-1} on a per H basis. This destabilization of the Ru surface accounts for a considerable portion of the activation barrier of the hydrogenation steps. The high barriers for O-H bond formations on the clean Ru surfaces could be reduced, if the assistance of water or methanol molecules would be considered on a clean surface[13] or if the surface coverage is included in the calculations as shown in the following sections.

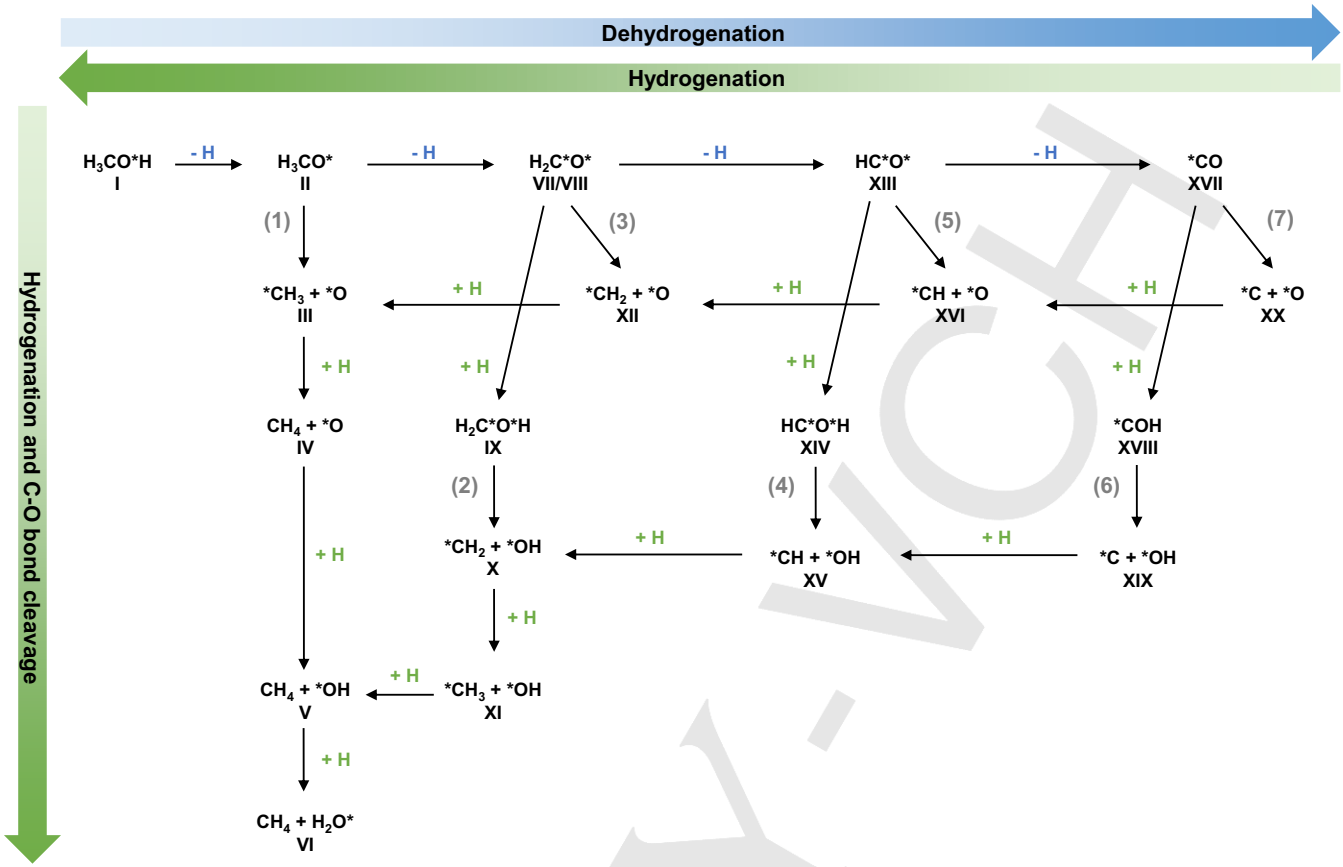

Scheme 4. Potential methanol decomposition pathways to methane. Adsorbed atoms are indicated by an asterisk. The different reaction pathways are numbered in brackets in gray. Roman numbers indicate the stationary points as shown in the energy profiles and structural images.

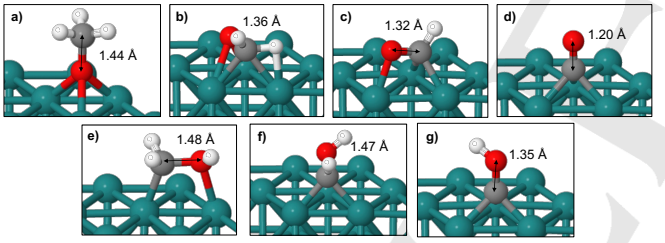

Figure 3. Adsorption geometries and C-O bond distances of a) CH_3O, b) CH_2O, c) CHO, d) CO, e) CH_2OH, f) CHOH and g) COH on a clean Ru(0001) surface.

In general, the stability of local minima increases with each dehydrogenation step of methanol and otherwise decreases after each hydrogenation reaction. This is due to the generation and consumption of hydrogen adsorbates in the reaction steps, which either stabilizes or destabilizes the surface afterwards (cf. Figure S16). This can be confirmed by the fact that for all investigated pathways the energetic span (ES, which is the difference between the highest transition state and the lowest intermediate and a measure for the total activation energy of a reaction pathway)[20] is determined by the TS of the water formation (V-VI), which represents the most hydrogenated stage in the catalytic cycle, and local minima at strongly dehydrogenated stages (Figures S8, S10, S13 and S16). A comparison of the ESs of the potential reaction pathways on the clean Ru model surface shows that the ES decreases, if the C-O bond cleavage takes place at an early dehydrogenation stage of methanol (Table 4). The reason is that less hydrogen adsorbates are formed at early dehydrogenation stages and thus, the surface is less stabilized, which would otherwise result in an increased ES.

Table 4. ESs of the methanol decomposition pathways on a clean Ru(0001) surface (without dispersion corrections).

CO cleavage of	ES [kJ mol^{-1}]
CH_3O **(1)**	166
CH_2OH **(2)**	133
CH_2O **(3)**	177
CHOH **(4)**	185
CHO **(5)**	223
COH **(6)** and CO **(7)**	242

The methanol decomposition pathways to methane via CH_3O **(1)**, CH_2OH **(2)** and CH_2O **(3)** C-O cleavage have the smallest ESs on the clean Ru surface and are therefore recalculated on a Ru(0001) surface saturated with hydrogen adsorbates to represent the experimental conditions and improve the computational results. Since hydrogen adsorbates showed a high mobility on the catalyst surface, H atoms are considered to migrate in or out of the investigated Ru slab in order to maintain

the most favorable hydrogen coverage on the catalyst surface. Consequently, the highest possible coverage of hydrogen is considered for each reaction step. If additional vacancies are required for the following reaction step, a migration of a vacancy from a different slab containing a vacancy is assumed, as the barrier is comparatively small (cf. Table 3). On the other hand, if a vacant site is generated in a reaction step, this vacant site is filled with a hydrogen adsorbate that migrates from another cell into the investigated slab.

In general, the mechanisms and the single reaction steps of the methanol decomposition on a Ru(0001) surface covered with hydrogen adsorbates are very similar compared to the clean surface. For all three investigated pathways, at first the methanol O-H bond is cleaved (i-ii) leading to a methoxy and a hydrogen atom. As an alternative to the surface-mediated cleavage of methanol, the concerted methanol O-H bond cleavage and recombination of the H atom with a surface hydrogen was probed (Figures S25-26). Since the repulsion between the adsorbates is too high on a fully hydrogen-covered surface, this reaction step was tested on a Ru slab with two vacant sites. However, the direct recombination of the methanol H with a surface hydrogen resulting in desorbed H_2 is less favorable than the homolytic cleavage of the methanol O-H bond. Following the decomposition pathway via CH_2OH C-O cleavage **(2)** (Figure 4), the formaldehyde species formed after the C-H bond cleavage of methoxy (vii) has to migrate on the surface to form the reactant geometry (x) of the following O-H bond formation. This migration coincides with the CH_2O rotation on the clean Ru model surface (cf. Figure S10) and the activation barriers are extremely low compared to the overall activation barrier (Figure S21). This again indicates that adsorbed molecules are quite mobile on the catalyst surface. Obviously stationary point x is less stable than vii since the CH_2O molecule is located in proximity to a H adsorbate. This repulsion can already be recognized from the fact that this hydrogen atom moves away from the threefold hollow to a bridge site (Figure S22). In contrast to the clean surface, the adsorption of one H_2 molecule that is required in the reaction does not take place at the beginning of the reaction, but most probably after the consumption of the hydrogen adsorbates that were generated from dehydrogenation of methanol. For pathway **(2)** via CH_2OH, this is the case after the hydrogenation of CH_2 to CH_3 (xiii). For all three investigated pathways, this leads to a fluctuating number of vacant sites by two in the course of the catalytic cycles.

When comparing the activation energies of the single reaction steps on the clean and the hydrogen-covered Ru(0001) surface, it becomes obvious that most barriers are comparable (Table 5). However, some hydrogenation reactions are facilitated significantly on the H-saturated surface (iii-iv, x-xi). This could be because many other hydrogen adsorbates can still stabilize the surface and repulsion can be reduced by forming an O-H or C-H bond. The activation barriers of O-H bond formations (iv-v, v-vi) however, are only slightly decreased on the hydrogen-covered surface. These TSs determine the ES for the pathways **(2)** and **(3)**. This leads to a smaller energetic span for the CH_2OH pathway **(2)** compared to CH_2O **(3)** since TS iv-v is slightly higher in energy than v-vi and the formation of OH from O (iv-v) can be avoided in pathway **(2)**. In addition, the ES for the CH_2OH pathway **(2)** is determined by stationary point v containing adsorbed OH, while the pathways via CH_2O **(3)** has a more stable intermediate with an adsorbed O atom (iv). Consequently, a reaction sequence that avoids the formation of O adsorbates and the formation of OH is the most favorable. For pathway **(1)** via CH_3O, the ES is very similar to pathway **(3)** (Table 6). However, the activation barrier determined by TS ii-iii of the C-O bond cleavage and the adsorbed O species has a slightly higher barrier (Figure S19). Among the three investigated reaction pathways on the H-covered Ru surface, the CH_2OH pathway **(2)** shows the best ES of 80 kJ mol^{-1} (Table 6) and is consequently the most probable reaction pathway. A separation of the Gibbs free energies of activation in enthalpic and entropic contributions reveals that the entropic contribution to the ES is quite small which is in accordance with the experimental result. This indicates that the rate-determining step does not include the adsorption or desorption of a molecule to or from the surface.

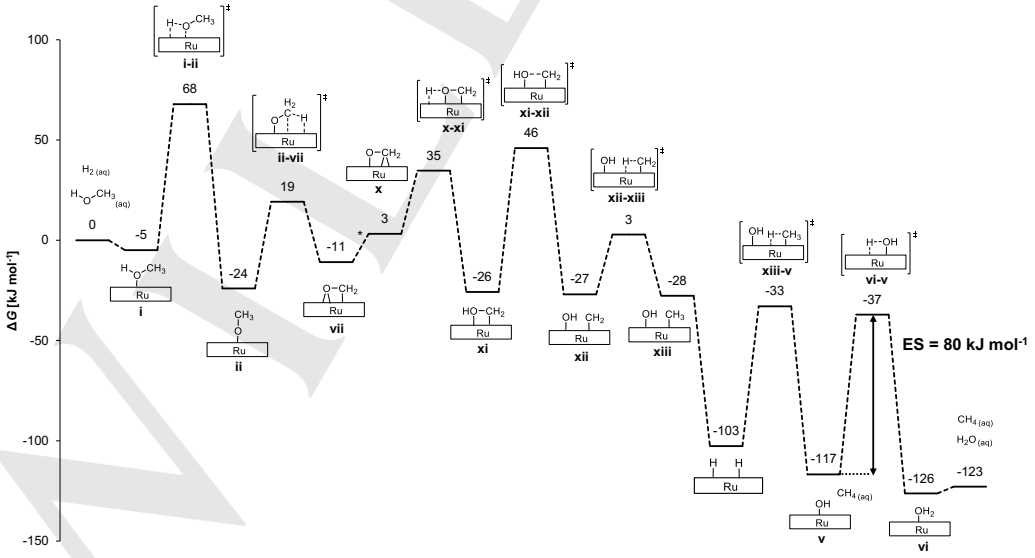

Figure 4. Energy profile of the methanol decomposition to methane on a H-saturated Ru(0001) surface via CH_2OH C-O cleavage **(2)**. *Corresponding stationary points can be found in Figure S21.

Table 5. Comparison of activation barriers of single reaction steps on the H-saturated ($\Delta G_{H\text{-}Sat.}$) and the clean Ru(0001) surface (ΔG_{clean}) (without dispersion corrections). Negative values indicate that the step is facilitated on the H-saturated surface. Values in brackets indicate the comparison between the clean surface without dispersion and the H-covered surface with dispersion.

Pathway	Reaction step	$\Delta G_{H\text{-}sat}$-ΔG_{clean} [kJ mol^{-1}]
CH_3O **(1)**	CH_3OH O-H cleavage (i-ii)	8 (3)
	CH_3O C-O cleavage (ii-iii)	-14 (-18)
	CH_4 formation (iii-iv)	-42 (-33)
	OH formation (iv-v)	-4 (-12)
	H_2O formation (v-vi)	-16 (-19)
CH_2OH **(2)**	CH_3O C-H cleavage (ii-vii)	-7 (-20)
	CH_2OH formation (x-xi)	-69 (-68)
	CH_2OH C-O cleavage (xi-xii)	12 (10)
	CH_3 formation (xii-xiii)	-25 (-16)
CH_2O **(3)**	CH_2O C-O cleavage (viii-xiv)	-10 (-14)
	CH_3 formation (xiv-iii)	-7 (-4)

Compared to the ESs of the respective mechanisms on the clean Ru surface, a reduction can be observed by considering hydrogen co-adsorbates on the catalyst surface. When comparing the ESs in Tables 4 and 6 it has to be mentioned that the ESs in Table 6 were calculated for cycles that contain dispersion corrections while the ESs of the pathways calculated in Table 4 do not. However, even without consideration of dispersion interactions the ES decreases by about 20 kJ mol^{-1} for the pathways via CH_3O **(1)** and CH_2OH **(2)** and by about 40 kJ mol^{-1} for the CH_2O pathway **(3)**. This effect can be explained by the fact that higher surface coverages result in lateral repulsive interactions.[10c] Consequently, the adsorbates are less stabilized on the surface, which reduces the activation barriers of the reaction steps.

Table 6. ESs of the decomposition pathways via CH_3O, CH_2OH and CH_2O C-O cleavages on a H-saturated Ru(0001) surface.

Pathway	ES [kJ mol^{-1}]	ΔH [kJ mol^{-1}]	ΔS [kJ mol^{-1}]
CH_3O **(1)**	133	128	-6
CH_2OH **(2)**	80	87	13
CH_2O **(3)**	127	129	5

Finally, a comparison of the computationally and experimentally determined activation barriers of the methanol hydrogenolysis reveals that ES of 80 kJ mol^{-1} on the H-saturated Ru(0001) surface via the CH_2OH intermediate is underestimated compared to the experimentally determined Gibbs free energy of activation ($\Delta G^{\ddagger}_{app}$ = 115 ± 10 kJ mol^{-1}). Possibly, the consideration of different crystal planes including steps and edges instead of the plane Ru(0001) surface could have an impact on the reaction. Furthermore, the approximations made for the entropic contributions could play a non-negligible role.

Nevertheless, periodic DFT is a suitable tool for the mechanistic analysis of this surface-catalyzed reaction. Moreover, this indicates that the consideration of the catalyst surface coverage is of high importance in order to obtain more reasonable energetic results.

Conclusion

To summarize, we reported a combined computational and experimental study on the Ru-catalyzed hydrogenolysis of methanol. A kinetics study on the methanol hydrogenolysis was performed on a Ru/C catalyst and gave a Gibbs energy of activation of $\Delta G^{\ddagger}_{app}$ = 115 ± 10 kJ mol^{-1}. As only methane was observed as a decomposition product experimentally, we investigated the methanol decomposition to methane on a Ru(0001) model surface using periodic DFT. In order to represent the reaction conditions, a surface modeling with different adsorbates was performed. The Ru surface saturated with hydrogen adsorbates is the most stable surface, though mixed water and hydrogen on the surface are relatively stable. Testing the mobility of adsorbed species revealed low migrational barriers for H and OH, while the mobility of O is limited. The reaction sequence of the methanol decomposition was examined on a clean Ru surface and on a Ru model surface saturated with hydrogen adsorbates. On a clean Ru surface, the ES of the reaction is lower if the methanol molecule undergoes fewer dehydrogenation steps before the C-O cleavage, since hydrogen adsorbates stabilize the metal surface and increase the ES. The smallest ESs were observed for the pathways via CH_3O, CH_2OH and CH_2O C-O cleavages. Generally, the mechanism on the H-saturated Ru catalyst is very similar to the clean surface. The activation barriers for the single reaction steps were comparable on the clean and the H-covered surface. However, several hydrogenation reactions are facilitated which could be explained by a reduced repulsion when O-H or C-H bonds are formed on the H-saturated Ru surface. On the Ru surface covered with hydrogen adsorbates, the CH_2OH pathway is the most favorable (80 kJ mol^{-1}), which is smaller than the experimentally determined Gibbs free energy of activation. Nevertheless, the results of this study emphasize the importance of modeling reactions under realistic conditions.

Based on the results of this publication, the hydrogenolysis mechanism of higher polyols such as ethylene glycol or glycerol can be investigated to elucidate the surface mechanism. In this regard, the dependence of the apparent activation energies on the position of the reacting group and the polyol chain lengths as observed previously[5b] can be examined.

Experimental and Computational Methods

Experimental Methods

Methanol (> 99.85%), acetic anhydride (> 97%) and pyridine (> 99%) were obtained from ChemSolute. Ru/C (5 *wt.*%) was obtained from Sigma-Aldrich. Molecular hydrogen (> 99.999%) was obtained from Linde. The hydrogenolysis of methanol was performed in high-pressure stainless steel autoclaves of 50 mL volume with a sampling tube equipped with a Teflon inlet and a magnetic stirrer. In a typical experiment, 0.525 g (16.4 mmol) methanol and 0.400 g Ru/C (5 *wt.*%) were added to the autoclave and dispersed in 20 mL water. After flushing the autoclave with

H_2, it was pressurized with 80 bar H_2. Subsequently, the autoclave was heated in an aluminum cone to reaction temperature (413 K, 423 K, 433 K, 443 K or 453 K) at a stirrer speed of 750 rpm. Samples were taken 0 min, 15 min, 30 min, 60 min, 120 min and 180 min after the reaction temperature was reached. The catalyst was filtered out over a polyamide filter with a pore size of 0.45 µm. 0.167 mL of the filtrate were dissolved in 2 mL acetic anhydride/pyridine (1:1 vol/vol). After stirring over night at room temperature, the samples were measured by gas chromatography (GC) [Thermo Scientific Trace GC system equipped with an Agilent DB-23 column (internal diameter: 0.25 mm; length: 60 m; film thickness: 0.25 mm; isobaric: 0.1 MPa He; temperature gradient: 353-527 K)]. Methanol was calibrated using the external standard method. All reactions were performed twice in order to prove reproducibility. The dispersion of the Ru/C catalyst was determined by a CO-pulse titration assuming a Ru:CO stoichiometry of 1:1. For an extensive characterization of the commercial Ru/C catalyst, the reader is referred to the publication by Haus et al.[21]

Determination of the Gibbs Energy of Activation

The rate constants of the methanol decomposition k_{mm} were calculated under the assumption of a pseudo-first order kinetics (Equation 1). For the fitting to the experimental data, an induction period at the beginning of the reaction is not considered in the fit, as the Ru/C catalyst most probably needs to be activated by an *in situ* reduction of the oxidic overlayer on the Ru surface. In addition, a certain time is needed until the reaction temperature is reached inside the autoclave.[5a] Therefore, the time zero was set 15-30 min after the beginning of the reaction. The methanol concentration was calculated numerically at intervals of 1 min. These concentrations were fitted to the experimental data by variation of k_{mm} by means of the MS Excel Solver Add-In with the solving method 'Generalized Reduced Gradient (GRG) non-linear' using the least square method.[5b]

$$\frac{dc_m}{dt} = -k_{mm} \cdot c_m \quad (1)$$

m: Methanol; mm: Methanol/methane

The second order rate constant k of the methanol decomposition is calculated by division of k_{mm} by the concentration of accessible Ru atoms c_{Ru} (Equation 2). c_{Ru} is determined according to Equation 3 considering the mass fraction of Ru (ω) and the metal dispersion (δ).

$$k = \frac{k_{mm}}{c_{Ru}} \quad (2)$$

$$c_{Ru} = \frac{m_{Ru/C} \cdot \omega_{Ru/C} \cdot \delta_{Ru/C}}{M_{Ru} \cdot V} \quad (3)$$

The apparent activation enthalpy $\Delta H^{\ddagger}_{app}$ and the entropy of activation $\Delta S^{\ddagger}_{app}$ were calculated using the Eyring method.[14] Therefore, a linear regression of $\ln {}^{k}/_{T}$ versus $1/T$ of the linearized form of the Eyring equation (Equation 4) was carried out. The Gibbs energy of activation $\Delta G^{\ddagger}_{app}$ was determined according to Equation 5. The standard error on $\Delta H^{\ddagger}_{app}$ and $\Delta S^{\ddagger}_{app}$ was calculated by division of the standard deviation by the square root of the number of data points. The standard error on $\Delta G^{\ddagger}_{app}$ is determined by a Gaussian error propagation of the errors on $\Delta H^{\ddagger}_{app}$ and $\Delta S^{\ddagger}_{app}$.

$$\ln\frac{k}{T} = \frac{-\Delta H^{\ddagger}}{R} \cdot \frac{1}{T} + \ln\frac{k_B}{h} + \frac{\Delta S^{\ddagger}}{R} \quad (4)$$

$$\Delta G^{\ddagger}_{app} = \Delta H^{\ddagger}_{app} - T \cdot \Delta S^{\ddagger}_{app} \quad (5)$$

Computational methods

All DFT calculations were carried out in a periodic framework using the VASP program series (revision 5.4.4)[22] combined with the PBE exchange-correlation functional[23] within the generalized-gradient approximation (GGA). In most cases, the PBE functional was complemented by the Grimme D3 correction with BJ damping[24] to account for dispersion. Preliminary studies such as the investigation of Ru hydrides, the estimation of migrational barriers and the study of catalytic cycles on a clean Ru surface do not contain dispersion corrections. This is indicated at the respective results. The electron-ion interactions were described by the PAW method.[25] In order to ensure accurate energies, the energy cut-off of the plane wave basis was set to 400 eV. The metal surface was modeled by a Ru(0001) slab, which is the thermodynamically most favorable surface.[26] A Ru-Ru distance of 2.71 Å was obtained from relaxation of Ru bulk. The slab consisted of a four-layered (3 x 3) cell of which the two top layers describing the surface were allowed to relax. The lower two layers were fixed during the optimization process to represent the bulk phase. The Brillouin-zone was sampled by a Γ-centered 7 x 7 x 1 Monkhorst-Pack grid[27] together with a second-order Methfessel-Paxton smearing of 0.2 eV.[28] In order to avoid interactions between slabs a 15 Å vacuum overlayer was implemented. Geometry optimizations of local minima on the potential energy surface were performed with convergence criteria for the electronic self-consistent energy and the ionic relaxation of 10^{-6} eV and 0.02 eV $Å^{-1}$, respectively. The TSs of minimum energy paths were localized by employing the NEB method[29] with four movable images between the fixed initial and final stationary points. Every TS was optimized with the improved dimer method[30] using a smaller convergence criterion for ionic relaxation of 0.01 eV $Å^{-1}$. Frequency calculations verified that every localized TS exhibits exactly one imaginary frequency corresponding to the investigated reaction step. Since the substrate methanol contains only one O atom that interacts with the surface, hydrogen bond interactions were assumed to be negligible in this study and therefore, solvation effects were calculated implicitly by using the VASPsol code[31] on preoptimized geometries. The zero-point energy and thermal contributions to the electronic energy were computed from frequency calculations of the free molecules and all adsorbates using statistical thermodynamics at a temperature of 150 °C and a pressure of 80 bar (see Supporting information).[32] Thermal contributions of adsorbed molecules and atoms were calculated according to the harmonic limit. Low-frequency modes of adsorbed systems below 100 cm^{-1} were shifted to 100 cm^{-1} for the calculation of the vibrational entropy and enthalpy to avoid a large error on the entropic terms. Adsorption energies G_{ads} were calculated using Equation 6, where G denotes the Gibbs energy of the isolated adsorbate (A), the clean Ru(0001) surface (Ru) or the adsorbed system (A/Ru).

$$G_{ads} = G_{A/Ru} - (G_A + G_{Ru}) \quad (6)$$

The activation barrier of the multistep reaction sequence is determined according to the ES model by Kozuch and Shaik.[20]

Acknowledgements

The authors kindly thank Heike Fickers-Boltz, Elke Biener and Hannelore Eschmann for the GC analyses. This study was performed as part of the Cluster of Excellence Fuel Science Center (EXC 2186, ID: 390919832) funded by the Excellence Initiative by the German federal state governments to promote science and research at German universities. NMS thanks RWTH Aachen University for financial support.

Keywords: Periodic density functional theory (DFT) • Heterogeneous Catalysis • Ruthenium • Methanol • Hydrogenolysis

References

[1] a) R. D. Perlack, *Biomass as Feedstock for a Bioenergy and Bioproducts Industry: The Technical Feasibility of a Billion-Ton Annual Supply*, Oak

Ridge National Laboratory, Oak Ridge, **2005**; b) A. M. Ruppert, K. Weinberg, R. Palkovits, *Angew. Chem. Int. Ed.* **2012**, *51*, 2564-2601.

[2] a) X. Liu, X. Wang, S. Yao, Y. Jiang, J. Guan, X. Mu, *RSC Adv.* **2014**, *4*, 49501-49520; b) C. Luo, S. Wang, H. Liu, *Angew. Chem. Int. Ed.* **2007**, *46*, 7636-7639; c) R. Palkovits, K. Tajvidi, J. Procelewska, R. Rinaldi, A. Ruppert, *Green Chem.* **2010**, *12*, 972-978; d) R. Palkovits, K. Tajvidi, A. M. Ruppert, J. Procelewska, *Chem. Commun.* **2011**, *47*, 576-578; e) Y. Liu, C. Luo, H. Liu, *Angew. Chem.* **2012**, *124*, 3303-3307.

[3] J. Zaffran, C. Michel, F. Delbecq, P. Sautet, *Catal. Sci. Technol.* **2016**, *6*, 6615-6624.

[4] a) D. Sohounloue, C. Montassier, J. Barbier, *React. Kinet. Catal. Lett.* **1983**, *22*, 391-397; b) C. Montassier, D. Giraud, J. Barbier, in *Stud. Surf. Sci. Catal., Vol. 41*, Elsevier, **1988**, pp. 165-170; c) M. A. Andrews, S. A. Klaeren, *J. Am. Chem. Soc.* **1989**, *111*, 4131-4133; d) C. Montassier, J. Menezo, L. Hoang, C. Renaud, J. Barbier, *J. Mol. Catal.* **1991**, *70*, 99-110; e) K. Wang, M. C. Hawley, T. D. Furney, *Ind. Eng. Chem. Res.* **1995**, *34*, 3766-3770; f) M. Mavrikakis, M. A. Barteau, *J. Mol. Catal. A* **1998**, *131*, 135-147.

[5] a) P. J. C. Hausoul, L. Negahdar, K. Schute, R. Palkovits, *ChemSusChem* **2015**, *8*, 3323-3330; b) P. J. C. Hausoul, A. K. Beine, L. Neghadar, R. Palkovits, *Catal. Sci. Technol.* **2017**, *7*, 56-63.

[6] a) L. Wright, L. Hartmann, *J. Org. Chem.* **1961**, *26*, 1588-1596; b) Á. Zsigmond, A. Kecskeméti, K. Bogár, F. Notheisz, E. Mernyák, *Catal. Commun.* **2005**, *6*, 520-524.

[7] R. García-Muelas, Q. Li, N. López, *ACS Catal.* **2015**, *5*, 1027-1036.

[8] A. S. Moura, J. L. C. Fajín, A. S. S. Pinto, M. Mandado, M. N. D. S. Cordeiro, *J. Phys. Chem. C* **2015**, *119*, 27382-27391.

[9] P. Gazdzicki, P. Jakob, *J. Phys. Chem. C* **2010**, *114*, 2655-2663.

[10] a) L. Di, S. Yao, S. Song, G. Wu, W. Dai, N. Guan, L. Li, *Appl. Catal., B* **2017**, *201*, 137-149; b) D. R. Alfonso, *J. Phys. Chem. C* **2013**, *117*, 20562-20571; c) N. K. Sinha, M. Neurock, *J. Catal.* **2012**, *295*, 31-44; d) T. Avanesian, G. S. Gusmão, P. Christopher, *J. Catal.* **2016**, *343*, 86-96.

[11] M. Garcia-Ratés, R. García-Muelas, N. López, *J. Phys. Chem. C* **2017**, *121*, 13803-13809.

[12] P. J. Feibelman, *Science* **2002**, *295*, 99-102.

[13] C. Michel, F. Auneau, F. Delbecq, P. Sautet, *ACS Catal.* **2011**, *1*, 1430-1440.

[14] H. Eyring, *J. Chem. Phys.* **1935**, *3*, 107-115.

[15] a) A. Michaelides, A. Alavi, D. King, *J. Am. Chem. Soc.* **2003**, *125*, 2746-2755; b) A. Hodgson, S. Haq, *Surf. Sci. Rep.* **2009**, *64*, 381-451.

[16] M. Chou, J. R. Chelikowsky, *Phys. Rev. B* **1989**, *39*, 5623.

[17] S. Gautier, P. Sautet, *J. Phys. Chem. C* **2017**, *121*, 25152-25163.

[18] N. V. Ilawe, J. A. Zimmerman, B. M. Wong, *J. Chem. Theory Comput.* **2015**, *11*, 5426-5435.

[19] J. Hrbek, R. A. DePaola, F. M. Hoffmann, *J. Chem. Phys.* **1984**, *81*, 2818-2827.

[20] S. Kozuch, S. Shaik, *Acc. Chem. Res.* **2011**, *44*, 101-110.

[21] M. O. Haus, Y. Louven, R. Palkovits, *Green Chem.* **2019**, *21*, 6268-6276.

[22] a) G. Kresse, J. Hafner, *Phys. Rev. B* **1994**, *49*, 14251; b) G. Kresse, J. Furthmüller, *Comput. Mater. Sci.* **1996**, *6*, 15-50.

[23] J. P. Perdew, K. Burke, M. Ernzerhof, *Phys. Rev. Lett.* **1996**, *77*, 3865.

[24] a) S. Grimme, J. Antony, S. Ehrlich, H. Krieg, *J. Chem. Phys.* **2010**, *132*, 154104; b) S. Grimme, S. Ehrlich, L. Goerigk, *J. Comput. Chem.* **2011**, *32*, 1456-1465.

[25] a) P. E. Blöchl, *Phys. Rev. B* **1994**, *50*, 17953; b) G. Kresse, D. Joubert, *Phys. Rev. B* **1999**, *59*, 1758.

[26] L. Vitos, A. Ruban, H. L. Skriver, J. Kollár, *Surf. Sci.* **1998**, *411*, 186-202.

[27] H. J. Monkhorst, J. D. Pack, *Phys. Rev. B* **1976**, *13*, 5188.

[28] M. Methfessel, A. Paxton, *Phys. Rev. B* **1989**, *40*, 3616.

[29] H. Jónsson, G. Mills, K. W. Jacobsen, in *Classical and Quantum Dynamics in Condensed Phase Simulations*, World Scientific, Singapore, **1998**, pp. 385-404.

[30] G. Henkelman, H. Jónsson, *J. Chem. Phys.* **1999**, *111*, 7010-7022.

[31] a) K. Mathew, R. Sundararaman, K. Letchworth-Weaver, T. A. Arias, R. G. Hennig, *J. Chem. Phys.* **2014**, *140*, 084106; b) M. Fishman, H. L. Zhuang, K. Mathew, W. Dirschka, R. G. Hennig, *Phys. Rev. B* **2013**, *87*, 245402.

[32] K. K. Irikura, D. J. Frurip, in *Computational Thermochemistry*, American Chemical Society, **1998**, pp. 402-418.

Entry for the Table of Contents

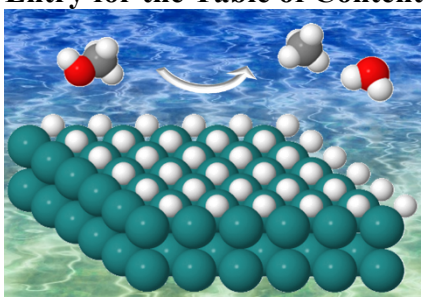

The hydrogenolysis of methanol on a ruthenium catalyst is studied computationally and kinetically to gain insights on the surface-catalyzed reaction. Using the periodic density functional theory, the reaction network of methanol to methane is investigated systematically considering coverage effects according to experimental conditions. The results serve as a basis for the hydrogenolysis of higher polyols in the future.

Institute and/or researcher Twitter usernames: @PalkovitsLab

WILEY-VCH